LA-UR- 08-4311

Approved for public release; distribution is unlimited.

Title: PAULI BLOCKING AND FINAL-STATE INTERACTION IN ELECTRON-NUCLEUS QUASIELASTIC SCATTERING

Author(s): Lon-chang Liu

Intended for: Physical Review C

Los Alamos
NATIONAL LABORATORY
EST. 1943

Pauli blocking and final-state interaction in electron-nucleus quasielastic scattering

Lon-chang Liu†

Theoretical Division, Group T-16, Mail Stop B243,

Los Alamos National Laboratory, Los Alamos, NM 87545 USA

(June 27, 2008)

The nucleon final-state interaction in electron-nucleus quasielastic scattering is studied. Based on the unitarity equation satisfied by the scattering-wave operators, a doorway model is developed to implement the Pauli-blocking of nucleon knockout. The model is complementary to the commonly used nuclear Fermi gas model which can not be applied with confidence to light- and medium-mass nuclei. Pauli blocking in these latter nuclei is illustrated with the case of Coulomb interaction. Significant effects are noted for beam energies below $\sim$ 350 MeV/c. Extension of the model to high-energy hadron-nucleus quasielastic scatterings is discussed.

† e-mail address: liu@lanl.gov

Keywords: Nuclear response function, Pauli blocking.

PACS:

I. INTRODUCTION

The dominant contribution to electron-nucleus reactions at energies below the pion production thrreshold comes from quasielastic electron-nucleus scattering, in which a target nucleon is knocked out to the continuum by the incoming electron. In the energy spectrum of the scattered electron, the quasielastic scattering gives a broad peak [1]. There are two classes of quasielastic experiments. In exclusive quasielastic experiments, both the outgoing electron and nucleon are measured and in coincidence. This class of experiments can provide detailed nuclear structure information of the struck nucleon [2]. On the other hand, in an inclusive quasielastic experiment, only the outgoing electron is measured. In other words, the energy and momentum of the knocked-out nucleon as well as the final state of the residual nucleus are not known specifically. Inclusive experiments cover the entire kinematic region down to a few MeV in the energy-loss spectrum of the electron. They allow us to check the consistency of various proposed nuclear reaction dynamics.

Since electromagnetic interaction is relatively weak, the distortion of the electron waves in the initial and final states can be ignored and only the interaction between the knocked-out nucleon and the residual nucleus (the nucleon final-state interaction) needs to be taken into account. In the literature, the potentials used to calculate the nucleon final-state interaction are energy dependent and complex valued. They differ, therefore, from the potential that binds the nucleon in the nucleus. Because eigenstates of different Hamiltonians are not orthogonal to each other, the nucleon scattering wavefunctions generated in the above-mentioned way are not orthogonal to the bound-state wavefunction of the nucleon.

This nonorthogonality between the wavefunctions leads to non-vanishing (spurious) contribution to nucleon knockout cross sections in the limit $\mathbf{q} \to 0$, where $\mathbf{q}$ is the momentum transfered to the nucleon. In the literature [3]— [5], various methods were proposed to remediate this lack of orthogonality. The same problem equally exists in theoertical calculations of an inclusive spectrum. A successful method has been developed with the use of Fermi-gas nuclear model. However, the application of Fermi gas to light and medium-mass nuclei is questionable. In this work, we show how to implement the orthogonality scattering in inclusive quasielastic scattering from light and medium-mass nuclei in a simple way.

We derive the model in Section II and give its application in Section III. Discussion and conclusions are summarized in Section IV.

II. ELECTRON QUASIELASTIC SCATTERING FROM A NUCLEUS

The one-photon exchange, one-nucleon knockout amplitude, $\mathcal{A}$, is illustrated in Fig.1. The 4-momenta of the on-shell particles (external lines of the diagram) are given by: $p_i = (E_i, \vec{p}_i)$ with $i = (0, 1, 2, C, A)$. In the laboratory frame, $p_A = (M_A, \vec{0})$. The 4-momentum of the photon is denoted by $q \equiv p_0 - p_2 = (E_0 - E_2, \vec{p}_0 - \vec{p}_2) \equiv (\omega, \vec{q})$. As in any Feynman diagram, the intermediate particles are off-mass-shell particles. This is the case with the intermediate photon, the intermediate nucleon, j, and the corresponding residual nucleus, denoted $C(j)$. However, it is useful to put the intermediate heavy nucleus, $C(j)$, on its mass shell. This covariant approximation enables one to use the bound-state nuclear wavefunctions given by traditional nuclear structure theories in which the negative-energy component of the wavefunction is not considered. [6] As a result, one has $p'_C = (E'_{C(j)}, \vec{p}\,'_C)$. Because the difference among various $M_{C(j)}$ is $\ll M_N$, it is useful to define M_C as an average of $M_{C(j)}$ and substitute the former for the latter. With the Bjorken-Drell convention [7] for the metric, single-particle state normalization, and reaction cross section, the quasielastic scattering differential cross section equals to

$$\frac{d^2\sigma}{d\Omega_2 dE_2} = \int \frac{(2\pi)^4}{v_{in}} \sum_{spins} \delta^3(\vec{p}_0 + \vec{p}_A - \vec{p}_1 - \vec{p}_2 - \vec{p}_C)\delta(E_0 + E_A - E_1 - E_2 - E_C)$$
$$\left(\frac{m_e M_A}{E_0 E_A}\right) \frac{1}{2(2J_A+1)} |\mathcal{A}|^2 \frac{|\vec{p}_2| E_2}{(2\pi)^3 (E_2/m_e)} \frac{d\vec{p}_1}{(2\pi)^3 (E_1/M_N)} \frac{d\vec{p}_C}{(2\pi)^3 (E_C/M_C)}\,, \quad (1)$$

where $v_{in} = E_0 E_A / \sqrt{(p_0 \cdot p_A)^2 - p_0^2 p_A^2}$ is the relative velocity in the initial channel, J_A is the spin of the target nucleus, and the summation is over the spin projections of the external particles. The amplitude $\mathcal{A}$ is shown graphically in Fig.1.

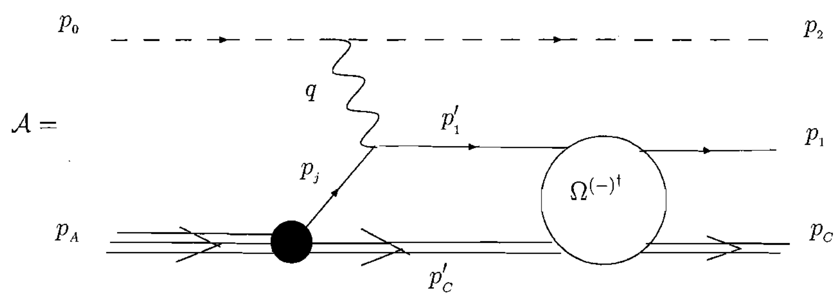

FIG. 1. Amplitude $\mathcal{A}$ for quasielastic scattering. The dashed, wavy, solid, and multiple solid lines represent, respectively, the electrons, the photon, the nucleon, and the nuclei. $\Omega^{(-)\dagger}$ is the wave operator for the nucleon final-state interaction. A summation over the target nucleon label j is understood.

Upon putting p_C' on its mass shell and keeping only the positive-energy spinors of the nucleon j, one obtains for amplitude $\mathcal{A}$ (see Fig.1):

$$\mathcal{A} = \left(\frac{ee_p f(q^2)}{q^2}\right) \overline{u}(\vec{p}_2, s_2)\gamma_\nu u(\vec{p}_0, s_0) \sum_{J_j\mu_j} \sum_{J_{C(j)}s_{C(j)}} \sum_{s_j s_1'} \int \frac{d\vec{p}_j}{(2\pi)^3 (E_j/M_N)(E_C'/M_C)(E_1'/M_N)}$$
$$\times \ \langle \vec{p}_1 \frac{1}{2} s_1;\ \vec{p}_C J_C s_C | \Omega_j^{(-)\dagger} | \vec{p}_1{}' \frac{1}{2} s_1';\ \vec{p}_C{}' J_{C(j)} s_{C(j)} \rangle \ \langle \vec{p}_1{}' \frac{1}{2} s_1' | \mathcal{J}^\nu(0) | \vec{p}_j \frac{1}{2} s_j \rangle$$
$$\times \left[\frac{\langle \vec{p}_j \frac{1}{2} s_j;\ \vec{p}_{C(j)}{}' J_{C(j)} s_{C(j)} | \Gamma | p_A J_A s_A \rangle}{p_j^0 - E_j + i\epsilon}\right] . \qquad (2)$$

Here the abbreviated notations $E_C' \equiv E_C(\vec{p}_C{}'), E_j \equiv E_N(\vec{p}_j)$ and $E_1' \equiv E_N(\vec{p}_1{}')$ are used. The 4-momentum consevation at each interaction vertex gives $\vec{p}_1{}' = \vec{p}_j + \vec{q}$, $\vec{p}_C{}' = \vec{p}_A - \vec{p}_j$, and $p_j^0 = E_A(\vec{p}_A) - E_C'(\vec{p}_C{}')$. The J_j, μ_j are the total angular momentum and its third component of the j-th target proton , and $\sum_{J_j\mu_j} = Z$ being the total number of the target protons. The e and e_p denote, respectively, the electron and proton charges, and the $u(\overline{u})$ and $U(\overline{U})$ the corresponding spinors. The $f(q^2)$ is the γpp form factor. In Eq.(2)

$$\langle \vec{p}_1{}' \frac{1}{2} s_1' | \mathcal{J}^\nu(0) | \vec{p}_j \frac{1}{2} s_j \rangle = \overline{U}(\vec{p}_1', s_1') \mathcal{J}^\nu(q) U(\vec{p}_j, s_j) = \int d\vec{x} \langle \vec{p}_1{}' \frac{1}{2} s_1' | e^{i\vec{q}\cdot\vec{x}} \mathcal{J}^\nu(\vec{x}) | \vec{p}_j \frac{1}{2} s_j \rangle \qquad (3)$$

where $\mathcal{J} = (\mathcal{J}^0, \vec{\mathcal{J}})$ is the electromagnetic current operator.

The quantity inside the square brackets in Eq.(2) is the covariant single-particle nuclear wavefunction. To see this, one notes that for the single-nucleon process shown in Fig.1, one can represent the target nucleus as an active nucleon i and a corresponding spectator residual nucleus $C(i)$, *i.e.*,

$$
\begin{aligned}
|\vec{p}_A J_A s_A\rangle &= \sum_{J_i J_{C(i)}} \mathcal{F}(J_i J_{C(i)}; J_A) \\
&\times \sum_{s_{C(i)}\mu_i} \mathcal{C}(J_i\mu_i,\ J_{C(i)} s_{C(i)}|J_A s_A) \sum_{m_i, s_i} \mathcal{C}(\frac{1}{2}s_i,\ \ell_i m_i|J_i\mu_i)\ \ |\frac{1}{2}s_i\rangle\, |\ell_i m_i\rangle\ |J_{C(i)} s_{C(i)}\rangle \\
&\equiv \sum_{\{i\}} |\Phi_{\{i\}}, \vec{p}_A J_A s_A\rangle\ . \qquad (4)
\end{aligned}
$$

Here $\mathcal{F}(J_i J_{C(i)}; J_A) \equiv [J_i^{\nu-1}(J_{C(i)})J_i J_A\ \ |\}\ \ J_i^\nu J_A]$ is the coefficient of fractional parentage, with ν being the number of protons in the shell having the momentum J_i. The $\mathcal{C}$'s are the Clebsch-Gordan coefficients. The $\{i\}$ stands for the ensemble of quantum numbers $J_i, \mu_i, J_{C(i)}, s_{C(i)}, s_i, \ell_i, m_i$. (Owing to parity conservation, only one ℓ_i is associated with a given J_i; hence, no summation over ℓ_i.) In a single-nucleon process, Γ acts only on the active nucleon. Consequently,

$$
\begin{aligned}
&\frac{\langle\vec{p}_j\frac{1}{2}s_j;\ \vec{p}^{\,\prime}_{C(j)} J_{C(j)} s_{C(j)}|\Gamma|\vec{p}_A j_A s_A\rangle}{p_j^0 - E_j + i\epsilon} \\
&= \mathcal{F}(J_i J_{C(i)}; J_A)\mathcal{C}(J_j\mu_j,\ J_{C(j)} s_{C(j)}|J_A s_A)\langle\vec{p}_j\frac{1}{2}s_j|\frac{1}{p_j^0 - E_j + i\epsilon}\Gamma|J_j\mu_j\rangle \\
&= \mathcal{F}(J_i J_{C(i)}; J_A)\mathcal{C}(J_j\mu_j,\ J_{C(j)} \mu_{C(j)}|J_A s_A)\langle\vec{p}_j\frac{1}{2}s_j|J_j\mu_j\rangle \\
&\equiv \Phi_{\{j\}}(\vec{\lambda}_j) \equiv \langle\vec{\lambda}_j|\Phi_{\{j\}}\rangle\ . \qquad (5)
\end{aligned}
$$

In obtaining the third line of the equation, the bound-state equation $G_0\Gamma\Phi_{bd} = \Phi_{bd}$ was used. From Eq.(4) one verifies easily

$$
\begin{aligned}
\Phi_{\{j\}}(\vec{\lambda}_j) &= \mathcal{F}(J_i J_{C(i)}; J_A)\mathcal{C}(J_j\mu_j,\ J_{C(j)} s_{C(j)}|J_A s_A)\ \mathcal{C}(\frac{1}{2}s_j,\ \ell_j m_j|J_j\mu_j)\ \Phi_{J_j\ell_j m_j}(\vec{\lambda}_j) \\
&= \langle\vec{p}_j\frac{1}{2}s_j|\Phi_{\{j\}}, \vec{p}_A J_A s_A\rangle \qquad (6)
\end{aligned}
$$

In Eqs.(1)-(6), the states $|\ \rangle$ and $\langle\ |$ are covariantly normalized, namely, $\langle\ \vec{k}', s'|\vec{k}, s\ \rangle = (E(\vec{k})/M)^{1/2}\delta(\vec{k}' - \vec{k}')\delta_{s's}$. On the other hand, in nonrelativistic nuclear theories the states are ususally not covariantly normalized. These latter states, denoted $|\ \rangle\rangle$ and $\langle\langle\ |$, have the normalization $\langle\langle\ \vec{k}', s'|\vec{k}, s\ \rangle\rangle = \delta(\vec{k}' - \vec{k})\delta_{s's}$. The relation between the covariant and nonocovariant states is $|\vec{k}\ \rangle = |\vec{k}\ \rangle\rangle\ (E(\vec{k})/M)^{1/2}$. It follows that the relation between Φ and its non-covariantly normalized counterpart, ϕ, is

$$\Phi_{\{j\}}(\vec{\lambda}_j) = \left(\frac{E_j E_{C(j)} E_A}{M_N M_C M_A}\right)^{1/2} \phi_{\{j\}}(\vec{\lambda}_j)\ , \tag{7}$$

where $\phi_{j_j\ell_j m_j}(\vec{\lambda}_j) \equiv R_{j_j\ell_j}(|\vec{\lambda}_j|)Y^{\ell_j}_{m_j}(\hat{\lambda}_j)$, and $\vec{\lambda}_j = \eta\vec{p}_j - \vec{p}\,'_{C(j)}/A = \vec{p}_j - \vec{p}_A/A$ with $\eta = (A-1)/A$ is the relative momentum between nucleon j and the corresponding residual nucleus $C(j)$. In the coordinates space, ϕ depends on the relative distance $\vec{x}$ between the nucleon j and the residual nucleus, namely, $\vec{x} = \vec{r}_j - \vec{r}_{C(j)}$. Hence, $\phi(\vec{x})$ is related to the single-particle shell-model wave function $\psi(\vec{r}_j)$ by $\phi(\vec{x}) = \eta^{-3/2}\psi(\vec{r}_j)$. [8] In the momentum space, one has $\phi(\vec{\lambda}_j) = \eta^{-3/2}\psi(\vec{p}_j)$.

Upon introducing Eqs.(2)-(6) into Eq.(1), one obtains

$$\begin{aligned}
\frac{d^2\sigma}{d\Omega_2 dE_2} &= \int \frac{(2\pi)^3}{v_{in}}\ \delta^3(\vec{p}_0 + \vec{p}_A - \vec{p}_1 - \vec{p}_2 - \vec{p}_C)\delta(E_0 + E_A - E_1 - E_2 - E_C)\ \frac{|\vec{p}_2|E_2}{(E_2/m_e)} \\
&\frac{e^2 e_p^2 |f(q^2)|^2}{(2\pi)^2 q^4}\left(\frac{m_e M_A}{E_0 E_A}\right)\frac{1}{2(2J_A+1)}\ \sum_{s_0 s_2}\left[\overline{u}(\vec{p}_0, s_0)\gamma_\mu u(\vec{p}_2, s_2)\overline{u}(\vec{p}_2, s_2)\gamma_\nu u(\vec{p}_0, s_0)\right] \\
&\sum_{\{j\},\{i\}}\int \frac{d\vec{p}_j d\vec{p}_i}{(2\pi)^6 (E_j/M_N)(E_i/M_N)}\left(\frac{M_C}{E'_{C(j)}}\right)\left(\frac{M_C}{E''_{C(i)}}\right)\left(\frac{{M_N}^2}{E_N(\vec{p}_j + \vec{q})E_N(\vec{p}_i + \vec{q})}\right) \\
&\frac{1}{2}\sum_{s'_1 s''_1}\langle\vec{p}_i\frac{1}{2}s_i\ |\mathcal{J}^\mu(0)|\ (\vec{p}_i + \vec{q})\frac{1}{2}s''_1\rangle\ \langle\ (\vec{p}_j + \vec{q})\frac{1}{2}s'_1\ |\mathcal{J}^\nu(0)|\ \vec{p}_j\frac{1}{2}s_j\rangle \\
&\times\ \Phi^*_{\{i\}}(\vec{\lambda}_i)\Phi_{\{j\}}(\vec{\lambda}_j)\quad \sum_{s_1 J_C s_C}\quad \langle\vec{p}_i + \vec{q}, \frac{1}{2}s''_1;\ \vec{p}\,''_C J_{C(i)} s_{C(i)}|\Omega_i^{(-)}|\vec{p}_1\frac{1}{2}s_1; \vec{p}_C J_C s_C\rangle \\
&\times\ \langle\vec{p}_1\frac{1}{2}s_1; \vec{p}_C J_C s_C|\Omega_j^{(-)\dagger}|\vec{p}_j + \vec{q}, \frac{1}{2}s'_1;\ \vec{p}\,'_C J_{C(j)} s_{C(j)}\rangle\frac{d\vec{p}_1 d\vec{p}_C}{(2\pi)^6 (E_1/M_N)(E_C/M_C)}\ .
\end{aligned} \tag{8}$$

Eq.(8) can be rewritten in the following compact form:

$$\frac{d^2\sigma}{d\Omega_2 dE_2} = \left(\frac{d\sigma_M}{d\Omega_2}\right)\left(\frac{m_e^2}{E_0 E_2}\frac{\mathcal{L}_{\mu\nu}\mathcal{W}^{\mu\nu}}{cos^2(\theta_2/2)}\right)\ . \tag{9}$$

Here, $\mathcal{L}$ is a second-order leptonic tensor defined by

$$\begin{aligned}
\mathcal{L}_{\mu\nu} &= \frac{1}{2}\ \sum_{s_0 s_2}\left[\overline{u}(\vec{p}_0, s_0)\gamma_\mu u(\vec{p}_2, s_2)\overline{u}(\vec{p}_2, s_2)\gamma_\nu u(\vec{p}_0, s_0)\right] \\
&= 2\left[\not{p}_{0\mu}\not{p}_{2\nu} + \not{p}_{2\mu}\not{p}_{0\nu} + g_{\mu\nu}(q^2/2)\right]/(4m_e^2)\ ,
\end{aligned} \tag{10}$$

and

$$\frac{d\sigma_M}{d\Omega_2} = \frac{\alpha^2}{4E_0^2}\frac{cos^2(\theta_2/2)}{sin^4(\theta_2/2)} = \frac{e^2 e_p^2}{(2\pi)^2}\frac{E_2^2}{q^4}cos^2(\theta_2/2) \tag{11}$$

is the Mott differential cross section, with $\alpha = e^2/(4\pi) = e_p^2/(4\pi)$ being the fine-structure constant. In obtaining the last equality in Eq.(11), the energy scale $E_0 \gg m_e, E_2 \gg m_e$ is used, so that $k_0 = E_0,\ k_2 = E_2$, and $q^2 = -4E_0E_2 sin^2(\theta_2/2)$.

The nuclear tensor $\mathcal{W}^{\mu\nu}$ equals, therefore, to

$$\mathcal{W}^{\mu\nu} = \int \frac{(2\pi)^3}{v_{in}}\ \delta^3(\vec{p}_0 + \vec{p}_A - \vec{p}_1 - \vec{p}_2 - \vec{p}_C)\delta(E_0 + E_A - E_1 - E_2 - E_C)\ \frac{|\vec{p}_2|M_A}{E_2 E_A}|f(q^2)|^2$$
$$\sum_{\{j\},\{i\}} \int \frac{d\vec{p}_j d\vec{p}_i}{(2\pi)^6 (E_j/M_N)(E_i/M_N)} \left(\frac{M_C}{E'_{C(j)}}\right)\left(\frac{M_C}{E''_{C(i)}}\right)\left(\frac{{M_N}^2}{E_N(\vec{p}_j + \vec{q})E_N(\vec{p}_i + \vec{q})}\right)$$
$$\frac{1}{2}\sum_{s'_1 s''_1} \langle \vec{p}_i \frac{1}{2} s_i\ |\mathcal{J}^\mu(0)|\ (\vec{p}_i + \vec{q})\frac{1}{2}s''_1\rangle\langle\ (\vec{p}_j + \vec{q})\frac{1}{2}s'_1\ |\mathcal{J}^\nu(0)|\ \vec{p}_j \frac{1}{2}s_j\rangle\ \Phi^*_{\{i\}}(\vec{\lambda}_i)\Phi_{\{j\}}(\vec{\lambda}_j)$$
$$\langle(\vec{p}_i + \vec{q})\frac{1}{2}s''_1;\ \vec{p}_C{}''J_{C(i)} s_{C(i)}|\Omega_i^{(-)}\mathcal{I}(1,C)\Omega_j^{(-)\dagger}|(\vec{p}_j + \vec{q})\frac{1}{2}s'_1;\ \vec{p}_C{}'J_{C(j)} s_{C(j)}\rangle \tag{12}$$

where

$$\mathcal{I}(1,C) \equiv \sum_{s_1 J_C s_C} \int |\vec{p}_1 \frac{1}{2}s_1; \vec{p}_C J_C s_C\rangle\langle\vec{p}_1\frac{1}{2}s_1; \vec{p}_C J_C s_C|\ \frac{d\vec{p}_1 d\vec{p}_C}{(2\pi)^6 (E_1/M_N)(E_C/M_C)} = 1\ , \tag{13}$$

as a result of the completeness of free two-particle states. Consequently, in Eq.(12)

$$\Omega_i^{(-)}\mathcal{I}(1,C)\Omega_j^{(-)\dagger} = \Omega_i^{(-)}\Omega_j^{(-)\dagger}\delta_{ij}. \tag{14}$$

The appearance of δ_{ij} is a consequence of one-step reaction process in which the residual nucleus acts as a spectator. Because the nucleon j and the residual nucleus can form bound states, the unitary equation of the wave operators is [9]

$$\Omega_i^{(-)}\Omega_j^{(-)\dagger}\delta_{ij} = (\ \mathbf{1} - \Gamma_j)\,\delta_{ij}\ , \tag{15}$$

with

$$\Gamma_j = \sum_{n=0}^{n_{max}} |n_{\{j\}}\rangle\langle n_{\{j\}}| \equiv \sum_n \Gamma_j^{(n)}\ . \tag{16}$$

Here, $\Gamma_j^{(n)}$ denotes the projector to the bound state $|n_{\{j\}}\rangle$, with $n = 0$ denoting the nuclear ground state and $n \neq 0$ the nucleon-emission-stable (NES) excited nuclear states. In the single-step reaction model, $|n_{\{j\}}\rangle = |J_j^{(n)}\rangle \otimes |J_{C(j)}\rangle$. Here, a nucleon j is lifted from its ground-state orbital (denoted J_j) to an excited orbital (denoted $J_j^{(n)}, n \neq 0$).

The projectors $\Gamma_j^{(n)}$ have the properties $\Gamma_j^{(n)} = \Gamma_j^{(n)\dagger}$ and $\Gamma_j^{(n)}\Gamma_j^{(m)\dagger} = \Gamma_j^{(n)}\delta_{nm}$. These properties allow us to rewrite Eqs.(15) and (16) as

$$\Omega_i^{(-)}\Omega_j^{(-)\dagger}\delta_{ij} = (\ \mathbf{1} - \Gamma_j)\,\delta_{ij} = \left(\mathbf{1} - \sum_{n=0}^{n_{max}} |n_{\{j\}}\rangle\langle n_{\{j\}}|\ \mathbf{1}\ |n_{\{j\}}\rangle\langle n_{\{j\}}|\ \right)\delta_{ij}\ . \tag{17}$$

This last equation defines the doorway-state model of final-state nucleon-nucleus interaction.

Using Eqs.(14)-(17) for the last line of Eq.(12), one obtains, after some angular-momentum recoupling algebra, that

$$\begin{aligned}\mathcal{W}^{\mu\nu} = \int \frac{d\vec{p}_1 d\vec{p}_C}{(2\pi)^3 v_{in}} \quad & \delta^3(\vec{p}_0 + \vec{p}_A - \vec{p}_1 - \vec{p}_2 - \vec{p}_C)\delta(E_0 + E_A - E_1 - E_2 - E_C)\frac{|\vec{p}_2|}{E_2}|f(q^2)|^2 \\ & \times (\ \Xi_I^{\mu\nu}\ -\ \Xi_{II}^{\mu\nu})\ ,\end{aligned} \tag{18}$$

with

$$\Xi_I^{\mu\nu} = \frac{1}{2}\sum_{s_1}\sum_{J_j\mu_j\ell_j m_j s_j} \langle\langle\ \vec{p}_j\frac{1}{2}s_j\ |\mathcal{J}^\mu(0)|\vec{p}_1\frac{1}{2}s_1\rangle\rangle\langle\langle\ \vec{p}_1\frac{1}{2}s_1\ |\mathcal{J}^\nu(0)|\ \vec{p}_j\frac{1}{2}s_j\rangle\rangle\ \ |\phi_{\{j\}}(\vec{\lambda}_j)|^2\ , \tag{19}$$

and

$$\begin{aligned}\Xi_{II}^{\mu\nu} = & \sum_{n=0}^{n_{max}}\frac{1}{2}\sum_{s's''}\sum_{J_j\mu_j\ell_j m_j s_j} |\phi_{\{j\}}^{(n)}(\vec{\lambda})|^2 \\ & \times\left[\int\frac{d\vec{p}_j}{(2\pi)^3}\ \phi_{\{j\}}^*(\vec{\lambda}_j)\ \langle\langle\ \vec{p}_j\frac{1}{2}s_j\ |\mathcal{J}^\mu(0)|\ (\vec{p}_j+\vec{q})\frac{1}{2}s''\ \rangle\rangle\ \phi_{\{j\}}^{(n)}(\vec{\lambda}_j+\eta\vec{q})\right] \\ & \times\left[\int\frac{d\vec{p}_i}{(2\pi)^3}\ \phi_{\{j\}}^{(n)*}(\vec{\lambda}_i+\eta\vec{q})\ \langle\langle\ (\vec{p}_i+\vec{q})\frac{1}{2}s'\ |\mathcal{J}^\nu(0)|\ \vec{p}_i\frac{1}{2}s_j\ \rangle\rangle\ \phi_{\{j\}}(\vec{\lambda}_i)\right]\ ,\end{aligned} \tag{20}$$

where $\vec{\lambda} = \eta\vec{p}_1 - A^{-1}\vec{p}_C$ is the relative momentum of the nucleon-residual nucleus system in the final state. Because of the momentum conservation at the γpp vertex, $\vec{\lambda} = \vec{\lambda}_j + \eta\vec{q}$. For succintness of notation, Eqs.(19) and (20) are expressed in terms of non-covariantly normalized nuclear wave functions $\phi_{\{j\}}$, and noncovariant states $\langle\langle\ |$ and $|\ \rangle\rangle$. Consequently, various normalization factors, of the form (E/M), are implicit. (See the discussion after Eq.(6).)

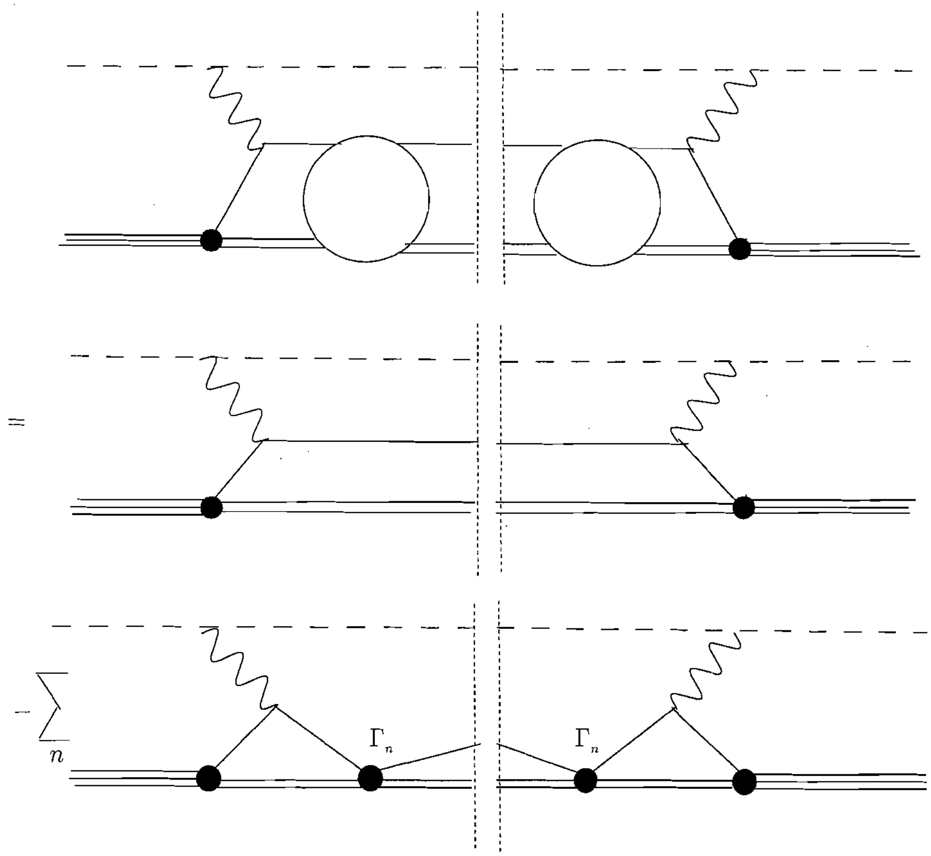

FIG. 2. The doorway-state model for Pauli-blocking corrections. As in Fig.1, the subscript j and a summation over it on both side of the graphic equation is implied.

Eq.(18) is illustrated in Fig.2. Its physics content is as follows. The Ξ_I leads to cross sections obtained with using plane waves in the final state. The Ξ_{II} gives the cross sections for the struck nucleon to remain bound. The subtraction of Ξ_{II} from Ξ_I corrects the spurious contribution arising from using plane waves. At $\vec{q}$=0, the subtraction is total, same as the orthogonality-scattering correction mentioned in section I.

Equations (18)-(20) also indicate that $\mathcal{W}^{\mu\nu}$ depends only on two independent four-vectors, p_A and q, where $q = (E_0 - E_2, \vec{p}_0 - \vec{p}_2) = (\omega, \vec{q})$. The most general Lorentz and gauge invariant second-order tensor has, therefore, the form [10], [11]

$$\mathcal{W}^{\mu\nu} = W_1(q^2, q \cdot p_A)\overline{g}^{\mu\nu} + W_2(q^2, q \cdot p_A)\frac{\overline{p}_A^{\mu}\overline{p}_A^{\nu}}{M_A^2} , \tag{21}$$

where

$$\bar{g}^{\mu\nu} = g^{\mu\nu} - q^{\mu}q^{\nu}/q^2 ,$$
$$\bar{p}^{\mu}_{A} = \left[p^{\mu}_{A} - (q \cdot p_A)\, q^{\mu}/q^2\right]/M_{A} . \tag{22}$$

Using the relations $q^{\mu}\mathcal{L}_{\mu\nu} = q^{\nu}\mathcal{L}_{\mu\nu} = 0$, and $p_{A} = (M_{A}, \vec{0})$ in the laboratory frame, one obtains

$$\left(\frac{m_e^2}{E_0 E_2}\mathcal{L}_{\mu\nu}\mathcal{W}^{\mu\nu}\right)_{lab} = W_2(q^2,\, q \cdot p_{A}) cos^2(\theta_2/2) - 2W_1(q^2,\, q \cdot p_{A}) sin^2(\theta_2/2) . \tag{23}$$

Consequently,

$$\left(\frac{d^2\sigma}{d\Omega_2 dE_2}\right)_{lab} = \frac{d\sigma_{M}}{d\Omega_2}\left[W_2(q^2,\, q \cdot p_{A}) - 2W_1(q^2,\, q \cdot p_{A}) tan^2(\theta_2/2)\right] . \tag{24}$$

Using the standard procedure [11], one can reexpress the functions W_1 and W_2 as a combination of two new functions X and Y, namely,

$$2W_1 = Y$$
$$W_2 = \frac{q^2}{|\vec{q}|^2} W_1 + \frac{q^4}{|\vec{q}|^4} X \tag{25}$$

where

$$X = \mathcal{W}^{00} = \int \frac{d\vec{p}_1 d\vec{p}_C}{(2\pi)^3 v_{in}}\; \delta^3(\vec{q} + \vec{p}_A - \vec{p}_1 - \vec{p}_C)\delta(\omega + E_A - E_1 - E_C)\; \frac{|\vec{p}_2|}{E_2}|f(q^2)|^2 \sum_{J_j \mu_j \ell_j m_j s_j}$$
$$\{ \left[\frac{1}{2}\sum_{s_1} \langle\langle\, \vec{p}_j \frac{1}{2} s_j\; |\mathcal{J}^0(0)| \vec{p}_1 \frac{1}{2} s_1 \,\rangle\rangle\; \langle\langle\, \vec{p}_1 \frac{1}{2} s_1\; |\mathcal{J}^0(0)|\; \vec{p}_j \frac{1}{2} s_j \,\rangle\rangle\; |\phi_{\{j\}}(\vec{\lambda}_j)|^2 \right]$$
$$- \left[\sum_{n=0}^{n_{max}} \frac{1}{2} \sum_{s' s''} \int \frac{d\vec{p}_j}{(2\pi)^3} \phi^*_{\{j\}}(\vec{\lambda}_j)\; \langle\langle\, \vec{p}_j \frac{1}{2} s''\; |\mathcal{J}^0(0)|\; (\vec{p}_j + \vec{q}) \frac{1}{2} s_j \,\rangle\rangle\; \phi^{(n)}_{\{j\}}(\vec{\lambda}_j + \eta\vec{q}) \right]$$
$$\left[\int \frac{d\vec{p}_i}{(2\pi)^3} \phi^{(n)*}_{\{j\}}(\vec{\lambda}_i + \eta\vec{q})\; \langle\langle\, (\vec{p}_i + \vec{q}) \frac{1}{2} s'\; |\mathcal{J}^0(0)|\; \vec{p}_i \frac{1}{2} s_j \,\rangle\rangle\; \phi_{\{j\}}(\vec{\lambda}_i) \right] \quad |\phi^{(n)}_j(\vec{\lambda})|^2 \quad \} . \tag{26}$$

The function Y has the same form as X but with the operator product $(\mathcal{J}^0)(\mathcal{J}^0)$ in X replaced by $\sum_{\lambda=\pm 1} (\vec{e}_{\vec{q},\lambda} \cdot \vec{\mathcal{J}})(\vec{\mathcal{J}}^{\dagger} \cdot \vec{e}^{\,\dagger}_{\vec{q},\lambda})$, where the $\vec{e}_{\vec{q},\lambda}$ are the spherical unit vectors defined with respect to the direction of the momentum transfer $\vec{q}$.

III. EFFECTS OF PAULI BLOCKING

To illustrate the effects of Pauli blocking correction (PBC), let us consider Coulomb scattering only. In this latter case, $\mathcal{J}^{\mu} = (\hat{\rho}, \mathbf{0})$. Hence, Y=0 and

$$\left(\frac{d^2\sigma}{d\Omega_2 dE_2}\right)_{lab} = \frac{d\sigma_M}{d\Omega_2}\frac{q^4}{|\vec{q}|^4}X \ . \tag{27}$$

The charge density operator $\hat{\rho}$ is given in the second quantization by

$$\hat{\rho}(\vec{x}) = \hat{\psi}^\dagger(\vec{x})\hat{\psi}(\vec{x}) \ . \tag{28}$$

In the nonrelativistic nuclear-structure theories, the two-component proton field is

$$\hat{\psi}(\vec{x}) = \int \frac{d\vec{k}}{(2\pi)^{3/2}} \sum_\xi e^{i\vec{k}\cdot\vec{x}} \ a_{\vec{k},\xi}\chi_\xi \ . \tag{29}$$

It follows that

$$\int \ e^{i\vec{q}\cdot\vec{x}}\hat{\rho}(\vec{x}) \ d\vec{x} = \sum_\xi \int \ d\vec{k} \ a^\dagger_{\vec{k}+\vec{q},\xi} \ a_{\vec{k},\xi} \ . \tag{30}$$

With the aid of Eq.(30), the two matrix elements of $\mathcal{J}^0$ in the first square brackets in Eq.(26) equal to $\delta_{s_1 s_j}$ while the two matrix elements of $\mathcal{J}^0$ in the second square brackets become, respectively, $\delta_{s'' s_j}$ and $\delta_{s' s_j}$. Consequently,

$$X = \int \frac{d\vec{K}}{v_{in}} \ \delta^3(\vec{q}+\vec{p}_A - \vec{K})\frac{|\vec{p}_2|}{E_2}|f(q^2)|^2 \ R(\omega,\vec{q}) \tag{31}$$

with

$$R(\omega,\vec{q}) = \delta(\omega + E_A - E_1 - E_C)\int \frac{d\vec{\lambda}}{(2\pi)^3}$$

$$\left[\sum_j \left(|\phi_{\{j\}}(\vec{\lambda}_j)|^2 - |\phi_{\{j\}}(\vec{\lambda})|^2 \ F^{00}_j(\vec{q})F^{00}_j(\vec{q})\right) - \sum_j{}' \sum_{n\neq 0} |\phi^{(n)}_{\{j\}}(\vec{\lambda})|^2 \ F^{0n}_j(\vec{q})F^{0n}_j(\vec{q})\right] \ . \tag{32}$$

In obtaining Eqs.(31) and (32) we used the relation $d\vec{p}_1 d\vec{p}_C = d\vec{K}d\vec{\lambda}$ with $\vec{K} \equiv \vec{p}_1 + \vec{p}_C$ and the relation

$$\int \frac{d\vec{p}_i}{(2\pi)^3}\phi^{(n)*}_{\{j\}}(\vec{\lambda}_i + \eta\vec{q}) \ \phi_{\{j\}}(\vec{\lambda}_i) = \int d\vec{r}_i \ e^{i\vec{q}\cdot\vec{r}_i} \ \psi^{(n)*}_{\{j\}}(\vec{r}_i) \ \psi_{\{j\}}(\vec{r}_i) = F^{0n}_j(\vec{q}) \ . \tag{33}$$

The $\sum{}'$ in Eq.(32) indicates that not every target proton is involved in a $0 \to n$ transition. Hence, $\sum_j{}' 1 \equiv Z' \leq Z$. The δ function in Eq.(32) constrains the energy loss ω. For example, in the nonrelativistic limit of kinematics this constraint gives $\omega = \vec{K}^2/(2M_1 + 2M_C) + \vec{\lambda}^2/(2m) + E_{sep}$, where $m \equiv M_1 M_C/(M_1 + M_C)$ is the reduced mass and $E_{sep} = M_1 + M_C - M_A$ is the average seperation energy of the target protons.

In Eq.(32), $F_j^{00}(\vec{q}) \equiv F_j^{g.s.\to g.s.}(\vec{q})$ is the nuclear (ground-state) form factor of the j-th proton with the property $F_j^{00}(0) = 1$. For $n \neq 0$, $F_j^{0n}(\vec{q}) \equiv F_j^{0\to n}(\vec{q})$ are the transition form factors, and $F_j^{0n}(0) = 0$. Consequently, when $\vec{q} \to 0$, $R(\omega, \vec{q}) \to 0$; *i.e.,* the knockout of a target proton is completely blocked at $\vec{q} = 0$. Because experimental form factors are parametrized with respect to the whole nucleus instead of to an individual proton, it is appropriate to define

$$\begin{aligned} F_j^{00}(\vec{q}) &= \frac{1}{Z} F_A^{00}(\vec{q}) \equiv F^{00}(\vec{q}) \; ; \\ F_j^{0n}(\vec{q}) &= \frac{1}{Z'} F_A^{0n}(\vec{q}) \equiv F^{0n}(\vec{q}) \quad (n \neq 0) \; . \end{aligned} \tag{34}$$

The q-dependence of PBC can be obtained by integrating over all energy loss in Eq.(32). With the aid of the normalization of the nuclear wave functions:

$$\int \frac{d\vec{\lambda}}{(2\pi)^3} |\phi_j(\vec{\lambda}_j)|^2 = \int \frac{d\vec{\lambda}_j}{(2\pi)^3} |\phi_j(\vec{\lambda}_j)|^2 = 1 \; , \tag{35}$$

we obtain

$$\begin{aligned} S(\vec{q}) &= \int d\omega \; R(\omega, \vec{q}) = Z \left(1 - [F^{00}(\vec{q})]^2 - \beta \sum_{n\neq 0}^{n_{max}} [F^{0n}(\vec{q})]^2 \right) \\ &\equiv Z L(\vec{q}) \; . \end{aligned} \tag{36}$$

The ratio $\beta \equiv Z'/Z$ depends on nuclear excitation mechanisms. The function $L(\vec{q})$ gives the probability for a struck proton to leave the nucleus. Eq.(36) highlights the difference between the doorway and Fermi gas models. In the Fermi gas model, the nucleon density distribution in the ground state, $|\psi(\vec{p}_j)|^2$, is assumed to be $\theta(|\vec{p}_j| - k_F)$ where k_F is the Fermi momentum. Because of Pauli principle, this box-type momentum distribution blocks $\psi(\vec{p}_j) \to \psi(\vec{p}_j + \vec{q})$ transitions for any momentum transfer $\vec{q}$ such that $|\vec{p}_j + \vec{q}| \leq k_F$. In a realistic nucleus, there is no such sharp momentum cutoff for Pauli blocking. In fact, the $\psi(\vec{p}_j)$ to $\psi^{(n)}(\vec{p}_j + \vec{q})$ transition probability is proportional to $[F^{0n}(\vec{q})]^2$. Hence, $[F^{00}(\vec{q})]^2 + \beta \sum_{n\neq 0} [F^{0n}(\vec{q})]^2$ is the probability that the struck nucleon remains bound and gives the Pauli-blocking correction to nucleon knockout in a realistic nucleus. We will soon see the marked difference between the PBC given by the doorway and Fermi gas models.

A comment on Eq.(36) is in order. While charge form factors F^{00} have been determined experimentally for a large number of nuclei, experimental information on transition form factors F^{0n} ($n \neq 0$) is much less systematic. However, in nuclei with mass number $A \leq 5$ there is no NES excited states. Consequently, only the term $[F^{00}(\vec{q})]^2$ is needed in Eq.(36). The $L(\vec{q})$ can, therefore, be calculated exactly for these light nuclei with the use of the measured charge form factors.

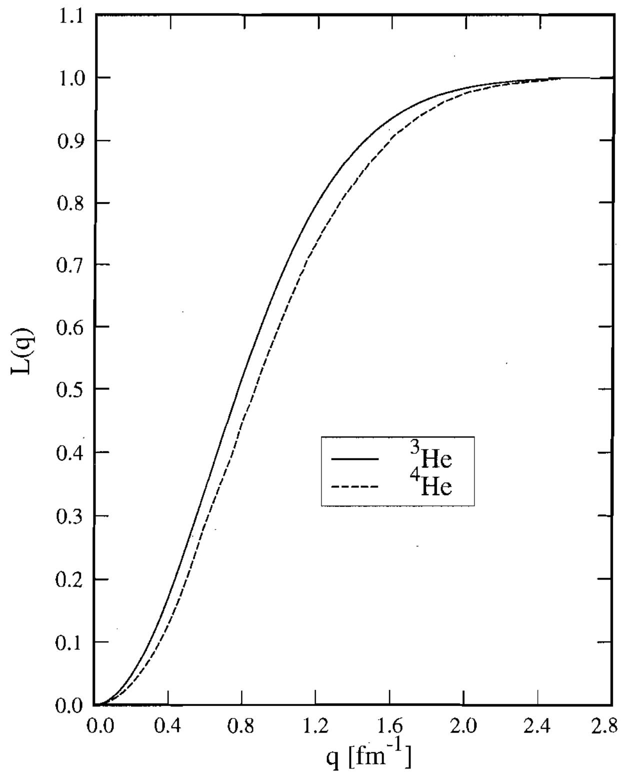

FIG. 3. Function $L(q) = 1 - [F^{00}(q)]^2$ for nuclei ^{3}He and ^{4}He.

In Fig.3, the functions $L(q) = 1 - [F^{00}(\vec{q})]^2$ for two light nuclei are shown. In both cases $L(q) = 0$ at $q = 0$ and , $L(q) \to 1$ when $q > 2.7\text{fm}^{-1}$. Graphically, the PBC is represented by $1 - L(q)$ which is the vertical distance between the curve and the horizontal line passing through $L(q)$=1. Fig.3 shows the PBC is complete *i.e.*, 100% at q=0. It further illustrates how PBC decreases with increasing q. . Since there is only one bound state in ^{3}He and ^{4}He (the ground states), $1 - [F^{00}(q)]^2$ represents an exact calculation of $L(q)$ for these nuclei.

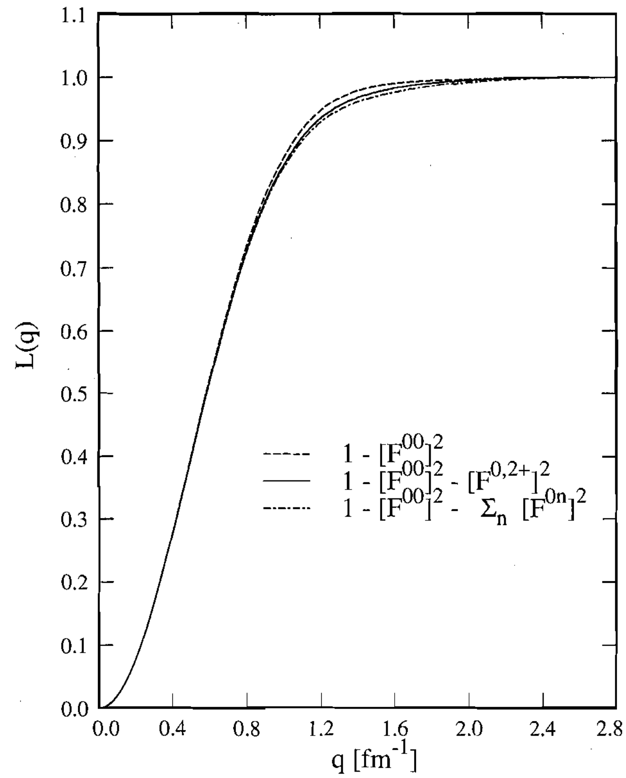

FIG. 4. Function $L(q)$ for ^{12}C. The $\sum_n$ includes transitions to NES states $2^+, 1^-, 3^-$, and 4^+.

In nuclei with mass number $A \geq 6$, there are NES states and its number increases with A. . To illustrate the effects of NES states in $1p$-shell nuclei, we show in Fig.4 the function $L(q)$ of ^{12}C, assuming $\beta = 1$ in Eq.(36). The PBC effects due to $[F^{00}]^2$ and $[F^{00}]^2$ + $[F^{0,2^+}]^2$ are given, respectively, by the dashed and solid curves in the figure. Here 2^+ is the 4.44 MeV ($T = 0$) excited state. The dot-dashed curve further includes the PBC arising from longitudinal transitions to the NES states [12]– [17] at 7.12 MeV ($1^-, T = 0$), 9.64 MeV ($3^-, T$=0), and 14.1 MeV ($4^+, T$=0). Since the proton seperation energy in ^{12}C is 15.11 MeV, the inclusion of these four states should take into account most of the NES transition strength. As one can see, the most important effects of $[F^{0n}]^2 (n \neq 0)$ comes from the longitudinal transition to the first 2^+ excited state at 4.44 MeV. The inclusion of other three states brings in only small additional effects. One could expect that, in general, only a limited number of transitions to NES states needs to be considered in medium-mass nuclei.

The relative importance of PBC effects due to different doorway channels can be evaluated from comparing the corresponding $\int L(q)dq$. We have found that $\int(1-[F^{00}(q)]^2)dq$ (integration of the dashed curve) differs from $\int(1-[F^{00}(q)]^2-\sum_n[F^{0n}(q)]^2)dq$, $(n = 2^+, 1^-, 3^-, 4^+)$ (integration of the dot-dashed curve) by less than 2%. In the following calculations of PBC in ^{12}C, we will, therefore, use the term $[F^{00}]^2$ only.

In Fig.5, we show PBC effects on inclusive quasielastic scattering cross sections at $E_0 = 200$ MeV and $\theta_2 = 60^o$ from ^{3}He and ^{12}C as a function of energy loss ω. For ^{12}C calculation an average separation energy $B = 25$ MeV was used. In Fig.6, we show PBC effects in these two nuclei at $E_0 = 500$ MeV and $\theta_2 = 60^o$. As one can see, the effects of PBC are significant at 200 MeV but negligible at 500 MeV.

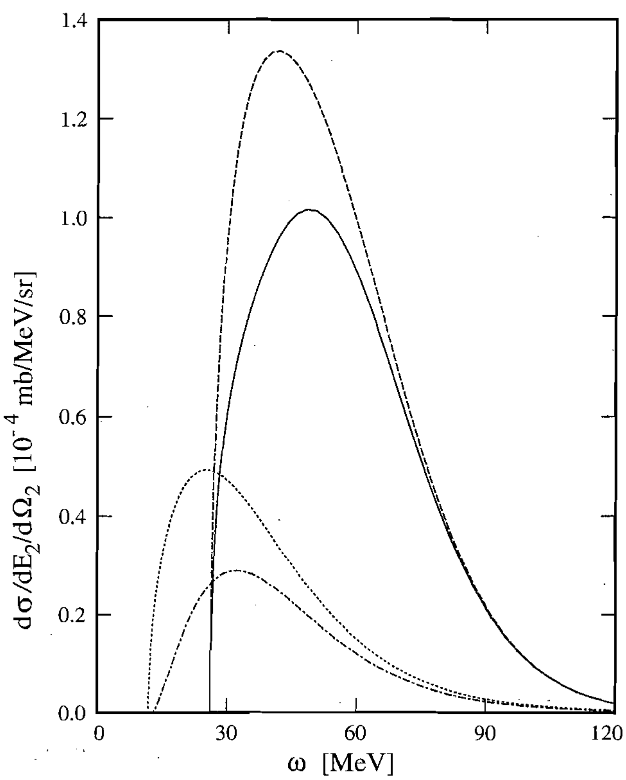

FIG. 5. Inclusive cross sections $(d\sigma/dE_2/d\Omega_2)_{lab}$ at $E_0 = 200$ MeV and $\theta_2 = 60^o$ as a function of energy loss ω. Dotted curve: ^{3}He without PBC; Dot-dashed curve: ^{3}He with PBC; Dashed cureve: ^{12}C without PBC; Solid curve: ^{12}C with PBC.

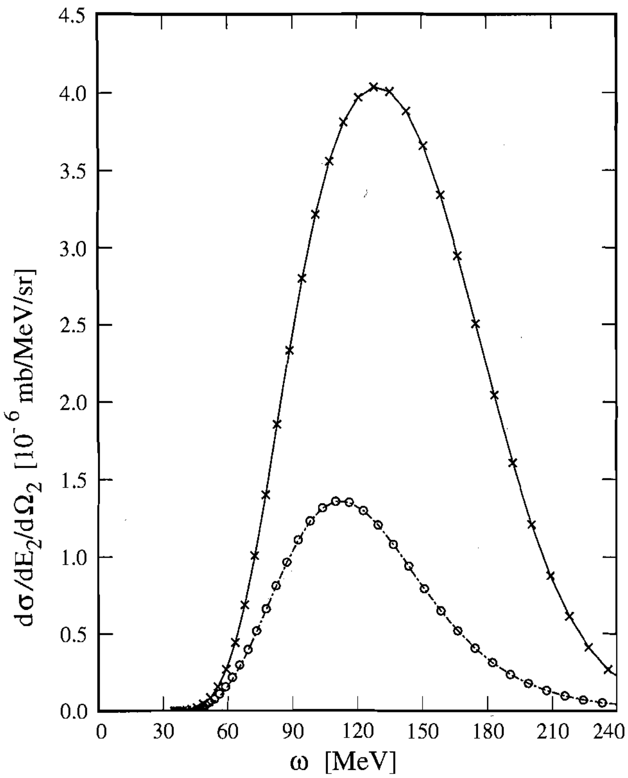

FIG. 6. Inclusive cross sections $(d\sigma/dE_2/d\Omega_2)_{lab}$ at $E_0 = 500$ MeV and $\theta_2 = 60^o$ as a function of energy loss ω. Circles: ^{3}He without PBC; Dot-dashed curve: ^{3}He with PBC; Crosses: ^{12}C without PBC; Solid curve: ^{12}C with PBC. Average separation energy used for ^{12}C.

To quantify the integrated PBC effects on the cross section, let us define

$$\delta = \frac{(d\sigma/d\Omega_2)^{noPBC} - (d\sigma/d\Omega_2)^{PBC}}{(d\sigma/d\Omega_2)^{noPBC}} \ . \tag{37}$$

The values of δ in ^{3}He and ^{12}C are given in Table I where a blank entry represents a δ <1 %. One can see that PBC increases with decreasing energy E_0 and scattering angle θ_2.

TABLE I. Pauli blocking correction δ [%].

E_0 [MeV]	^{3}He: $\theta_2 = 30^o$	$\theta_2 = 45^o$	$\theta_2 = 60^o$	^{12}C: $\theta_2 = 30^o$	$\theta_2 = 45^o$	$\theta_2 = 60^o$
200	78	58	40	63	37	18
350	44	18	6	21	3	
500	18	3		3		

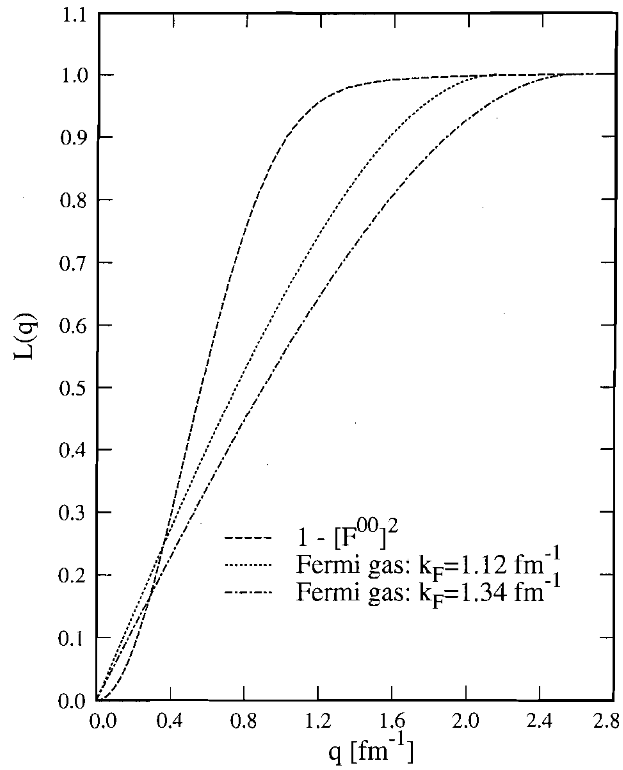

FIG. 7. Functions $L(q)$ given by doorway and Fermi gas models for ^{12}C.

In heavy-mass nuclei, the number of NES excited states becomes very large. In addition, very little is known about these states individually. It becomes, therefore, necessary to use the Fermi-gas nuclear model to calculate PBC. For a nonrelativistic Fermi gas, the probability for a nucleon to occupy the unoccupied levels situated above the Fermi momentum k_F is [11]

$$\begin{aligned} L(q) &= 1 && ;q \geq 2k_F \\ &= \frac{3}{2}\left(\frac{q}{2k_F}\right) - \frac{1}{2}\left(\frac{q}{2k_F}\right)^3 && ;q \leq 2k_F \ . \end{aligned} \tag{38}$$

($L(q)$ equals to the function $S^{in}(q, k_F)/Z$ in ref. [11].) Eq.(38) shows that in Fermi gas model, $L(q)$ depends only on k_F. Hence, $L(q)$ does not contain information of any finer aspect of nuclear structure. In Fig.7, we compare the $L(q)$ given by the doorway PBC model using realistic ^{12}C nuclear wave function (dashed curve) with those given by the Fermi-gas model having different k_F (dotted and dot-dashed curves) . As we can see, the Fermi-gas model gives less PBC at $q < 0.3$ fm^{-1}, but greater PBC at intermediate q's. This difference reflects the effect of nuclear structure.

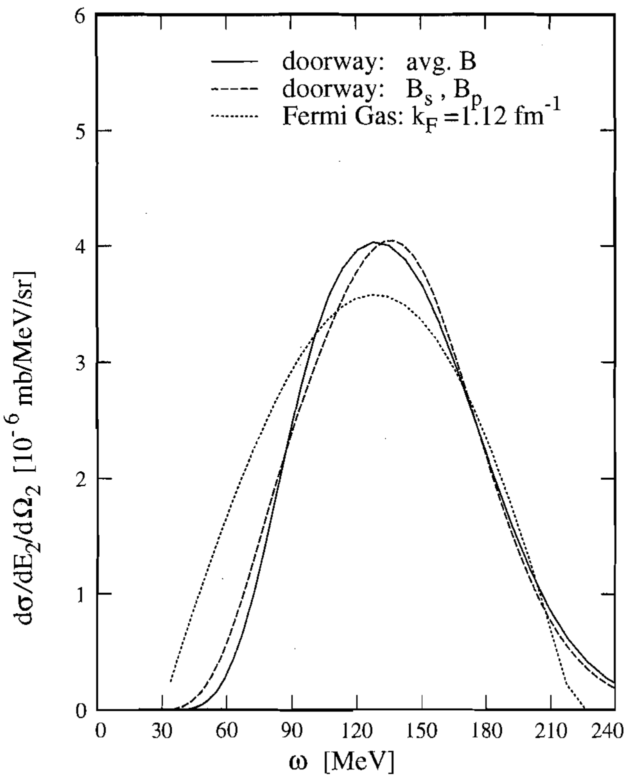

FIG. 8. Cross sections of quasielastic scattering from ^{12}C at $E_0 = 500$ MeV and $\theta_2 = 60^o$.

In the literature [19], upon treating k_F as a free parameter, a good fit to inclusive electron quasielastic scattering from ^{12}C at $E_0 = 500$ MeV and $\theta_2 = 60^o$ was obtained with an average nucleon separation energy, which we denote B, equal to 25 MeV and with a $k_F = 1.12$ fm^{-1} (the standard value of k_F is 1.34 fm^{-1}.) In Figs. 8 and 9, we compare the lab. cross sections of quasielastic scattering from ^{12}C at $\theta_2 = 60^0$, and at $E_0 = 500$ and 200 MeV, respectively. The dotted curves are given by Fermi gas model having the same parameters as those of ref. [19], *i.e.*, B=25 MeV and $k_F = 1.12$ fm^{-1}. The solid curves are given by the doorway model having the same average separation energy B=25 MeV. The dashed curves are also due to doorway model but with realistic separation energies $B_p = 15$ and $B_s = 35$ MeV respectively for the $1p$- and $1s-$ shell protons in ^{12}C. One notes that the difference between the cross sections given by the Fermi gas and doorway models are relatively small at 500 MeV (Fig. 8) but significant at 200 MeV (Fig. 9). At $E_0 = 500$ MeV and $\theta_2 = 60^o$ the average momentum transfer is > 2.4 fm^{-1}, it follows that PBC is negligible. Hence, the difference between the various ω-dependences of the cross sections in Fig. 8 is due mainly to the use of different nucleon momentum distributions in Fermi gas and doorway models.

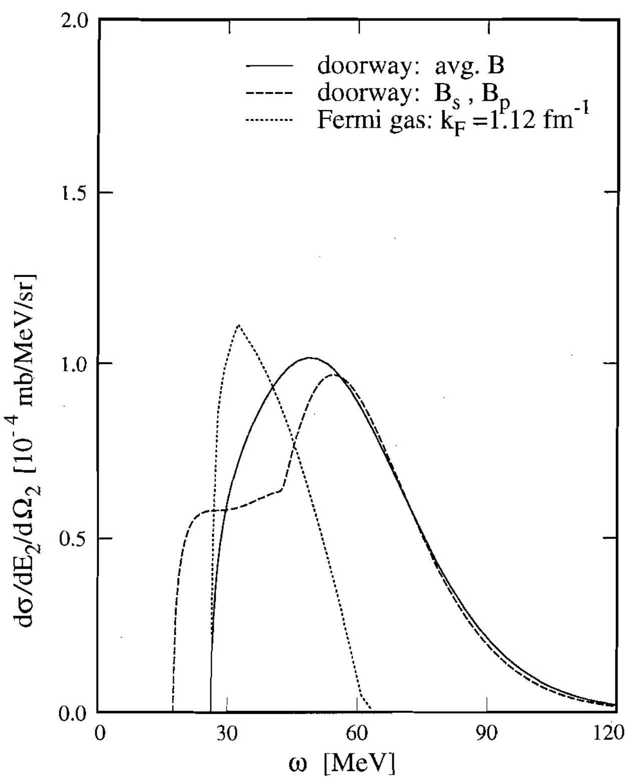

FIG. 9. Cross sections of quasielastic scattering from ^{12}C at $E_0 = 200$ MeV and $\theta_2 = 60^o$.

This apparent similarity disappears, however, at 200 MeV (Fig. 9). The rapid decrease of cross sections shown by the dotted curve at $\omega > 60$ MeV arises from the step-function nucleon momentum distrbution with $k_F = 1.12$ fm^{-1} in the Fermi gas model. This ω-dependence of the cross sections is in marked difference with those given by the doorway model (solid and dash-dotted curves) where the use of realistic nucleon momentum distribution leads to a more gradual PBC. In addition, the use of realistic shell-dependent proton seperation energies in the doorway model predicts that at 200 MeV the contributions to cross sections arising from the $1s-$ and $1p-$ shells proton begin to seperate from each other in the spectrum. This valuable information cannot be given by the Fermi gas model. Fig. 9 indicates, therefore, that Fermi gas becomes an inadequate representation of nucleon momentum distribution in ^{12}C.

IV. DISCUSSION AND CONCLUSIONS

The doorway model can be easily extended to treat final-state interaction in inclusive hadron-nucleus quasielastic scattering from nuclei. For hadron-nucleus quasielastic scattering at high energies ($E_0 > 1$ GeV), the probability that the scattered high-energy hadron and the residual nucleus to form bound states is almost zero. Consequently, as long as the residual nucleus is not measured, plane wave can be used, to a very good approximation, to describe the scattered hadron. In addition, at very high energies the spin-flip part of the hadron-nucleon interaction is negilgible with respect to the spin-nonflip part. As a result, high-energy hadron-nucleon amplitude can be treated as spin-independent [18]. This leads to a situation similar to Coulomb scattering in electron-nucleus quasielastic scattering, namely, only the density operator $\hat{\rho}$ is relevant to the Pauli blocking. However, owing to the strong hadron-nucleus interaction, the distortion of the incoming hadronic wave function must be taken into account. In fixed-scatterer approximation to the hadron-nucleus quasielastic scattering Eq.(33) retains its basic formal structure but with the following replacements:

$$\begin{aligned} \phi_{\{j\}}(\vec{\lambda}_j) &\longrightarrow \phi^{DW}_{\{j\}}(\vec{\lambda}_j) \equiv \int d\vec{p}\,'\; \chi^{(+)}_{\vec{p}}(\vec{p}\,')\phi_{\{j\}}(\vec{\lambda}_j)\;; \\ F^{0n}(\vec{q}) &\longrightarrow F^{0n}_{DW}(\vec{q}) \equiv \int d\vec{\lambda}_j \phi^{(n)^*}_{\{j\}}(\vec{\lambda}_j + \eta\vec{q})\; \phi^{DW}_{\{j\}}(\vec{\lambda}_j)\;; \\ \sum_{j=1}^{Z} &\longrightarrow \sum_{j=1}^{A}\,, \end{aligned} \tag{39}$$

where $\chi^{(+)}_{\vec{p}}(\vec{p}\,')$ is the distorted wavefunction of the incoming hadron, which can be calculated with an optical model and eikonal approximation. The $\vec{p}$ and $\vec{p}\,'$ denote, respectively, the relative momenta between the hadron probe and the target nucleus in the initial state and in the intermediate state prior to the direct hadron-nucleon collision that knocks out the nucleon. In Eq.(39) the momentum $\vec{\lambda}_j$ depends on $\vec{p}\,'$, namely, in the hadron-nucleus c.m. frame $\vec{\lambda}_j = -\eta\vec{p}\,' - \vec{p}_C$. Accordingly, the first term of Eq.(32) is to be replaced by $\sum_j (2\pi)^{-3} \int d\vec{\lambda} |\phi_{\{j\}}^{DW}(\vec{\lambda}_j)|^2 \equiv A_{eff}$ with $A_{eff} < A$.

The orthogonality-scattering approaches proposed in the literature make use of optical potentials to model the nucleon-residual nucleus interaction. However, for some nuclear states of a residual nucleus the corresponding nucleon optical potential is not known. The present approach is less model-dependent, because the inputs to the calculation are the experimentally determined form factors. Consequently, the doorway approach to nucleon-nucleus final-state interaction represents a useful alternate to the orthogonality-scattering formalism proposed in the literature.

While at the present time the application of the doorway model to heavy-mass nuclei is hindered by the lack of a systematic experimental knowledge of the NES transition form factors in these nuclei, it does have advantages over the Fermi gas model in evaluating Pauli blocking correction in medium-mass and light nuclei. Firstly, the doorway model can incorporate realistic nuclear structure while the Fermi gas model cannot. Secondly, while a large number of nucleons in a heavy-mass nuclei may be represented by a nucleonic gas, the adequacy of treating a small number of nucleons as a structureless gas is certainly questionable. We have seen that for carbon (A=12), the Fermi gas representation becomes already inadequate. For nuclei with mass numbers $A \leq 5$, the doorway calculation is exact. For $1p-$shell nuclei such as ^{12}C the model can be calculated to a very good approximation with only using the measured ground-state (g.s.) nuclear form factor. One could expect that this latter approximation equally holds for $1d-$ and $1f-$shell medium-mass nuelci. Further studies are called for. We have seen that at 500 MeV the doorway and Fermi gas model give qualitatively similar results. In other words, in inclusive quasielastic scatterings the detailed nuclear structure information begin to be washed out as the beam energy increases. On the other hand, as the beam energy decreases the nuclear structure effect becomes important. In summary, the doorway formalism of Pauli blocking of spurious nucleon knockout is less model dependent than the usual orthogonality scattering approach, it incorporates nuclear structure effects, and can be readily applied to light and medium-mass nuclei.

REFERENCES

[1] Herbert Uberall, *Electron Scattering from Complex Nuclei*, Academic Press, New York and London (1971), pp.703-747.

[2] L.S. Celenza, W.S. Pong, M.M. Rahman, and C.M. Shakin, *Phys. Rev. C* **26** (1982) 320.

[3] Q. Haider and J.T. Londergan, *Phys. Rev. C* **23** (1981) 19.

[4] J. Noble, *Phys. Rev. C* **17** (1978) 2151.

[5] Louis S. Celenza and C.M. Shakin, *Phys. Rev. C* **20**, (1979) 385.

[6] L. Celenza, L.C. Liu, and C.M. Shakin, *Phys. Rev. C* **11** (1975) 1593, appendix B.

[7] J.D. Bjorken and S.D. Drell, *Relativistic Quantum Mechanics*, McGraw-Hill Book Co., New York (1964).

[8] L.C. Liu and C.M. Shakin, *Nuovo Cim.* **53A**. 142 (1979).

[9] Leonard S. Rodberg and R.M. Thaler, *Introduction to the Quantum Theory of Scattering*, Academic Press, New York and London, 1967, p.182.

[10] S.D. Drell and J.D. Walecka, *Ann. Phys. (N.Y.)* **28** (1964) 18.

[11] John Dirk Walecka, *Electron Scattering for Nuclear and Nucleon Structure*, Cambridge University Press, 2001.

[12] J.B. Flanz, R.S. Hicks, R.A. Lindgren, G.A. Peterson, A. hotta, B. Parker, and R.C. York, *Phys. Rev. Lett.***41**, 1642 (1978).

[13] Y. Torizuka, M. Oyamada, K. Nakahara, K. Sugiyama, Y. Kojima, T. Terasawa, K. Itoh, A. Yamaguchi, and M. Kimura, *Phys. Rev. Lett.***22**, 544 (1969).

[14] A. Nakada, Y. Torizuka, and Y. Horikawa, *Phys. Rev. Lett.* **27** 745 (1971), errata: **27**, 1102 (1971).

[15] R.M. Haybron, M.B. Johnson, and R.J. Metzger, *Phys.Rev.* **156**, 1136 (1967).

[16] Hall Crannel, *Phys. Rev.***148**, 1107 (1966).

[17] I. Ahmad, *J. Phys. G***3**, 1327 (1977).

[18] P.H. Hansen and A.D. Krisch, *Phys.Rev.D***15**, 3287 (1977).

[19] E.J. Moniz, L. Sick, R.R. Whitney, J.R. Ficenec, R.D. Kephart, and W.P. Trower, *Phys. Rev. Lett***26**, 445 (1971).